Accepted Manuscript

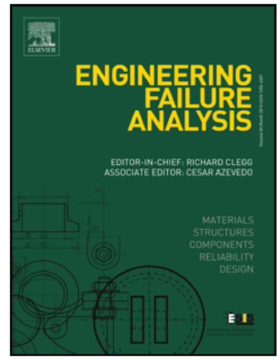

Numerical analysis of pile-soil system under seismic liquefaction

M. Saeedi, M. Dehestani, I. Shooshpasha, G. Ghasemi, B. Saeedi

PII:	S1350-6307(17)30627-1
DOI:	doi:10.1016/j.engfailanal.2018.07.031
Reference:	EFA 3561
To appear in:	*Engineering Failure Analysis*
Received date:	16 May 2017
Revised date:	15 May 2018
Accepted date:	23 July 2018

Please cite this article as: M. Saeedi, M. Dehestani, I. Shooshpasha, G. Ghasemi, B. Saeedi , Numerical analysis of pile-soil system under seismic liquefaction. Efa (2018), doi:10.1016/j.engfailanal.2018.07.031

Numerical analysis of pile-soil system under seismic liquefaction

M. Saeedi[a], M. Dehestani[b]*, I. Shooshpasha[c], G. Ghasemi[a], and B. Saeedi[a]

[a] Graduate Student, Faculty of Civil Engineering, Babol Noshirvani University of Technology, Babol, Iran

[b] Corresponding Author, Associate Professor, Faculty of Civil Engineering, Babol Noshirvani University of Technology, Babol, Iran

[c] Associate Professor, Faculty of Civil Engineering, Babol Noshirvani University of Technology, Babol, Iran

[*] The corresponding authors' address for future correspondence is:

Mehdi Dehestani

Associate Professor, Faculty of Civil Engineering

Babol Noshirvani University of Technology, Babol

Postal Box: 484, Babol

Postal Code: 47148-71167, I.R. Iran

Tel/Fax: +981132331707

Email: dehestani@nit.ac.ir

Abstract

This study considers the motion of an end bearing single pile with lumped mass embedded in sandy soil deposit subjected to seismic liquefaction. An efficient finite difference model, whose accuracy was validated through experimental results, has been constructed to study the dynamic responses of piles under liquefaction. Effects of parameters such as soil and pile properties, and predominant frequency on dynamic response of pile are examined. Results reveal that earthquake predominant frequency, pile stiffness, soil relative density and soil-pile relative stiffness, can significantly affect the pile's dynamic response, while pile material densities have negligible effects. Final results demonstrate that with increasing in pile stiffness, soil relative density and soil-pile relative stiffness, maximum moments in piles are increased while with increasing the earthquake predominant frequency, maximum moments in piles and depth of the liquefaction are reduced. Also, the depth in which the maximum value of moment, M_{max}, occurs, depends only on the pile stiffness.

Keywords: Pile; Liquefaction; Bending Moment; Seismic loading;

1. Introduction

When Pile foundations are exposed to intense dynamic transverse loads during earthquakes, soil–structure interaction (SSI) plays an important role in allocating the response of pile foundations to lateral excitation [1]. Recent observations after major earthquakes have shown that extensive damages and destructions are still likely to be happened to pile foundations. This problem is important particularly for pile foundations in loose saturated cohesionless deposits which are vulnerable to liquefaction and lateral spreading during seismic loading. Design procedures that have been developed for evaluating pile behavior under earthquake loading, have many uncertainties to be used for cases involving liquefaction. The performance of piles in liquefied soil layers is much more complex than that of non-liquefying soil layer as a result of the diminishing of stiffness and shear strength of the surrounding soil over time due to the increase of pore water pressure [2].

Lateral loads on piles are developed by the superstructure inertia as well as the soil movement induced by wave propagation through the soil. Inertial forces are the predominant forces before liquefaction and are mainly responsible for development of maximum bending moment near the pile head, whereas, kinematic forces which are predominant after liquefaction are responsible for the maximum bending moment observed at the interface of liquefiable and non-liquefiable layers [3]. However, consideration of the mentioned forces simultaneously, could lead to a more accurate analysis. This is due to the fact that the total forces are resulted from an inertial interaction from the oscillation of the superstructure and also a kinematical interaction from the soil deformation and motion.

Tokimastu and Suzuki [4] believe that the peak pile bending moment in the pile with respect to natural period of structure and natural period of ground can be estimated by Square-Root-of-Sum-of-Squares (SRSS) or algebraic addition of kinematic and inertial moment.

The complexity of the dynamic soil-pile-structure interaction is attributed to high degree of the coupling between the modes and the components of the interaction. In recent decades, an extensive range of laboratory tests and numerical approaches has been implemented for the purpose of providing a better understanding of the dynamic behavior of pile foundations in liquefiable soils. Pile foundation behavior in liquefiable soil depends on numerous parameters, including soil type, earthquake parameters, and pile properties.

Ishihara [5] used nonlinear 3-D analysis to show the importance of factors such as inertial interaction, kinematic interaction, seismic pore water pressures, soil nonlinearity, cross stiffness coupling and dynamic pile to pile interaction which typically is neglected in approximate methods in practice.

Wilson et al. [6] conducted a series of centrifuge tests on single piles and pile groups located in liquefiable soils in order to observe the p–y behavior of piles embedded in liquefying sands.

Bhattacharya [7] have evaluated two pile failure mechanisms in fourteen centrifuge tests, and concluded that before lateral spreading of the liquefied soil, slender pile sections face the buckling instability and may fail due to buckling before the action of lateral forces of moving liquefied soil. Further, he pointed out that pile length, diameter, and material strength can affect failure mechanisms of piles. The experimental results by Tang and Ling [8] have shown that decreasing the frequency and increasing the amplitude of earthquake excitation increase the pile bending moment and expedite excess pore pressure buildup in the free-field. Several researches on dynamic behavior of pile foundations in liquefiable soils were carried out utilizing shaking table tests [9, 10 11, 12, 13, 14, and 15].

Bhattacharya et.al [16] after quantitative reappraisal the collapse of Showa bridge, concluded that by increasing the unsupported length of the pile due to liquefaction, the natural period of the bridge tuned with the period of the liquefied ground causing resonance which caused excessive deflection at the pile head.

A number of researchers developed one-dimensional Winkler method for the seismic analysis of piles based on finite element or finite difference methods and liquefaction of surrounding soil was taken into account during analyzing process [17, 18, 19, and 20], while others used three-dimensional finite element method in for simulating piles in layered liquefying soil [2, 22, 23, 24 and 25]. Each of these models possesses varying prediction accuracy and certainty. In some of these papers fully-coupled formulation has been employed; while in others the uncoupled formulation, in which soil skeleton displacements and pore water pressure generation were computed separately, has been used.

Liyanapathirana and Poulos [20] modeled piles in liquefying soil with dynamically loaded beam on Winkler foundation and stated that the significance inertia force at the pile head, that depends on the superstructure mass and the acceleration of the superstructure, increases with the increase in relative density that reduce the degree of soil liquefaction and enabling large accelerations to be transmitted through the ground to the superstructure.

Haldar and Babu [26] investigated failure mechanisms of pile foundations in liquefiable soil using a nonlinear constitutive model for soil liquefaction, strength reduction, and pile-soil interaction and performed a parametric study on pile behavior for different pile, earthquake, and soil characteristics. In their study the effect of superstructure inertia has been taking into account by applying a horizontal load about 10% vertical load of the superstructure with a constant direction.

1.1. Research significance

The major objective of this research work is to study the interaction of soil-pile systems (SPS) considering both kinematic and inertia effects on SPS response. The kinematic effect of ground and the inertial interaction effect are evaluated simultaneously, and are combined in dynamic numerical model. In this study, the bending behavior of pile foundations embedded in different soils are analyzed using a finite difference program, known as Fast Lagrangian

Analysis of Continua (FLAC) [27]. Soil liquefaction is taken into consideration utilizing a nonlinear constitutive model (Byrne, 1991) [28]. For the validation of the constitutive model, centrifuge test results obtained from the literature [6]. For examining the response of a single end bearing pile in liquefiable soil, four different earthquake predominant frequency values, three different ranges of soil relative densities, and concrete and steel tube piles with six different diameters are considered.

2. Model description

Dynamic liquefaction analysis is performed by a two-dimensional, plain strain model in FLAC based on an explicit finite difference scheme. Analysis of soil-structure interaction is possible by coupling FLAC formulation to the structural element model. Damping and energy-absorbing characteristics of real soil are captured using the hysteresis curves for sandy soil.

The dynamic loadings are applied as acceleration time histories to the base of the model. Wave reflections at model boundaries are minimized by specifying free-field boundary conditions, which cause the outwards waves to be absorbed properly, at the two sides of the model.

The selection of mesh size for the FLAC dynamic model is conducted based on Kuhlemeyer and Lysmer [29] formula, to ensure accurate wave transmission. For providing reasonable runtime, the maximum frequency that can be modeled accurately is

$$f_{max} = \frac{V_s}{10\Delta L} \tag{1}$$

where Vs, and ΔL are the shear wave velosity, and the maximum dimensions of mesh, respectively. By filtering the history and removing high frequency components, a bigger mesh size may be used without remarkabely affecting the results.

Pore pressure generation in FLAC can be modeled by built-in constitutive model, namely the Byrne model [33]. The Byrne model for modeling the soil considers soil behavior due to energy dissipation, volume changes and modulus degradation under cyclic loading. The constitutive model as proposed by Byrne is a simplification of the Finn model and is

$$\frac{\Delta\varepsilon_{vd}}{\gamma} = C_1 \exp\left(-C_2\left(\frac{\varepsilon_{vd}}{\gamma}\right)\right) \tag{2}$$

where $\Delta\varepsilon_{vd}$ is incremental volume strain; ε_{vd} is accumulated volume strain; γ is cyclic shear strain amplitude; C_1 and C_2 are constants and can be obtained by using an empirical relation between relative density, D_r , and normalized SPT-N value with overburden pressure of 100 kPa and corrected to a ratio of 60%, $(N1)_{60}$:

$$C_1 = 7600(Dr)^{-2.5} \tag{3}$$

$$Dr = 15\sqrt{(N1)_{60}} \tag{4}$$

$$C_2 = \frac{0.4}{C_1} \tag{5}$$

Soil is modeled using Mohr-Coulomb model and the pile is modeled using two nodded linear elastic pile elements with interface properties and each element has three degrees of freedom (two displacements and one rotation) at each node.

Basically, the analysis of piles is a 3D problem. However, Donovan et al. [30] suggested linear scaling of material properties in order to distribute the discrete effect of elements over the distance between elements in a regularly spaced pattern. Piles are modeled as pile elements and soil-pile interface properties. Normal and shear stiffnesses are scaled to represent plane strain conditions using the Donovan et al. scale factor. Hence, plain strain analysis is conducted in the present study for the analysis of the single pile response under seismic loadings.

Inertia effects under seismic loading have been incorporated in dynamic model by defining a lumped mass placed on pile head as superstructure. Inertia effects in previous studies by FLAC

[26] have been considered by applying a horizontal load equal to 10% of the vertical load on pile. In the analysis, it is considered that the free head pile is founded on bed rock and there is no possibility of settlement during earthquake shaking and liquefaction.

The shear and normal stiffnesses of springs at pile-soil interface are assigned in the FLAC model as suggested by Comodromos et al. [36]:

$$k_n \ or \ k_s = 10 \times max\left[\frac{k+\frac{4G}{3}}{\Delta z_{min}}\right] \tag{6}$$

where k_n. k_s, K and G are shear and normal stiffnesses the bulk and shear moduli, respectively; and ΔZ_{min} is the smallest width of an adjoining zone in the normal direction.

2.1. Model Validation

Response of pile and soil modeled in finite difference program is validated using centrifuge test data reported by Wilson et al. [6]. Model in test consisted of two horizontal layers of saturated, fine, and uniformly graded Nevada sand. The lower layer is of 11.4 m thickness with 80% of relative density (*Dr*) and the upper layer is of 9.1 m thickness with 55% of relative density. A steel pipe pile with outer diameter of 0.67 m and 0.019 m wall thickness is extended up to 3.8 m above the ground surface and embedded up to 15 m below ground surface with a superstructure load of 480 kN. Kobe (1995) earthquake time history data [6] with scaled peak acceleration of 0.22 g is used for the centrifuge test. A baseline correction is adopted for the acceleration time history and the input horizontal acceleration is applied at the boundaries of the model. The characteristics of two layered soil medium and pile properties as adopted in the centrifuge test are given in Table 1. The shear modulus of the soil deposit is computed from the paper by Popescu and Prevost [32]:

$$G = G_{max} \frac{\left(\frac{1+2K_0}{3}\right)\sigma'_{v0}}{p_0} \tag{7}$$

where K_0 is coefficient of lateral earth pressure at rest; p_0 stands for the reference normal stress (100 kPa); and G_{max} represents low strain shear modulus of the soil.

The lateral dimension is adopted as 40 m for the analysis. Total soil medium is discretized into 750 finite difference grids in 30 rows and 25 columns. The pile is divided into 20 equal segments. Figure 1 illustrates the schematic diagram of the finite difference model.

Computed results for pore water pressure distribution, and bending moment history of pile are demonstrated in Fig. 2 and Fig. 3, respectively. Figure 2 shows excess pore water pressure from the centrifuge model and finite difference model. It is evident that the numerical model predicts the measured excess pore water pressure reasonably well. As shown in Fig. 3, a comparison between the bending moment time histories and those of centrifuge tests for the depth of 2.3 m reveals that the results from the two-dimensional plain strain finite difference model and centrifuge test data match sufficiently well. Hence in the following parametric study, the above finite difference model can be employed for assessing the response of single pile foundation in liquefied sandy soil.

3. Problem statement

In order to study the influences of soil and pile parameters on pile-soil interaction during lateral seismic loading and liquefaction, a series of fully coupled nonlinear dynamic analyses have been conducted. Three various soil different relative densities 40%, 55%, and 80% are considered which have shear modulus ranging from 25000 kPa to 41460 kPa. The depth of the soil layer is considered to be 20 m and the lateral dimension of the soil environment in dynamic model is 40 m and is discretized to 600 numbers of 4-noded quadrilateral finite difference grids (30 rows and 20 columns). The water table is assumed to be at the ground level.

A 21-m end bearing pile with various radiuses varying from 0.6 to 1 m is considered. Pile sections are made from concrete or steel, and the length of the pile above the ground is assumed equal to 1 m. The piles are modeled with pile elements in FLAC. The total length of modeled piles below ground is 20 m.

A superstructure mass of 740 kN is placed on single pile's top, which is taken from the vertical load of Showa bridge's pile. The elastic modulus and the density of the lumped mass are 20 GPa, and 96093 kg/m^2, respectively. The lumped mass is modeled with a cylindrical object with diameter and height of 1m. Figure 4 illustrates the schematic configuration of the finite difference models.

Four different earthquake time history data are utilized for the analysis which capture a wide range of frequencies from 1.2 to 5 Hz and are scaled to 0.1g, 0.2g, and 0.3g. Linear baseline corrected scaled earthquake data are used.

According to the elastic properties listed in Table 2, the least shear wave velocity is 118 m/s and largest zone size is 1.33 m. Therefore, according to the equation (1) this choosing of mesh size will not affect the result provided that the input acceleration's allowable frequencies are less than 8.8 Hz. Because of a fall of shear wave velocity in soil under dynamic loading, frequencies above 8.5 Hz are removed in this model.

The depth of liquefiable soil and maximum bending moment (M_{max}) are evaluated from the analysis. The characteristics of pile, soil, and earthquakes are given in Tables 2, 3, and 4.

4. Results and Discussion

The influences of different soil relative densities, pile stiffness, pile material densities, soil-pile relative stiffness for four earthquake predominant frequencies and three peak acceleration values, on the pile's dynamic response are examined as follows.

4.1. Depth of Liquefied Soil Layer

In saturated sandy soil, due to seismic excitation and subsequently high shear strains in soil layer, pore water pressure increases at different soil depths. Excess-pore water pressure ratios (Ru) at different times of excitation at different depths of soil are obtained. When Ru reaches a value near 1.0 the soil is considered to be completely liquefied thus the depth from which Ru becomes near 1 is the depth of liquefaction (H_L). Evaluations are accomplished due to dynamic loads pertaining to four earthquakes listed in Table 4 with scaled maximum accelerations of 0.1g, 0.2g, and 0.3g.

The evaluated depths of liquefied layer for different soil and earthquake parameters are presented in Fig. 5. According to Fig. 5, it is evident that increase in predominant earthquake frequency decreases the depth of liquefaction, because of deviating from fundamental frequency of liquefied soil which is followed by lower applied shear [26]. Furthermore, it can be concluded that with increase in soil density, the depth of liquefaction decreases, which is expected. Decrease in depth of liquefaction decreases the free length of pile as well as the natural period of pile system.

4.2. Effect of soil relative density

Relative density of saturated sand (D_r) is playing a significant role in determining pile response during seismic excitation. Higher relative densities following with higher $(N_1)_{60}$ and friction angels (φ), lead to increase in soil bearing capacity, and reduction of improper subsidence.

Besides, the probability of liquefaction under dynamic shakings is lower for denser soil medium. Therefore it can be considered to reduce buckling instability under severe dynamic loadings conditions. Effects of variations in sandy soil's relative densities on pile dynamic response and induced internal forces have been examined by applying earthquake motions to boundaries of models with four different relative densities: 40% (loose sand), 55% (medium dense sand), and 80% (dense sand).

The maximum bending moment (M_{max}) values for different soil relative densities (D_r) and two peak acceleration values (a_{max}= 0.1g and 0.3g) in four earthquakes for one meter of diameter concrete and steel pile sections are evaluated and presented in Fig. 6. According to Fig. 6, increase in soil relative density results in higher M_{max}. For example, M_{max} of the concrete pile with 1 meter diameter in soil with relative density of 40%, 55%, and 80% are obtained as 1000, 1250, and 1500 kN.m, respectively under Kocaieli earthquake with the maximum scaled acceleration of 0.1g. Other pile sections have been considered in 216 analyses and eventually in 87.8% of cases a fairly similar general trend was observed. In 12.2% of cases, the increase in soil relative density did not cause increment in M_{max} for four earthquake frequencies. It may be noteworthy to state that most of the non-obeying trends pertained to Kocaeli, earthquake.

The evaluation of obtained results has shown that, Mmax for piles under Kocaeli earthquake with amax=0.2g, in soils with the relative densities of 40% and 55% occurred in 22.2 and 22.8s. Mmax in these soils under scaled shaking acceleration of amax=0.3g have occurred in 20.5 and 22.8 s, whereas the peak acceleration of earthquake occurred at 14 s.

In contrast for soil with the relative density of 80% Mmax and earthquake peak acceleration occurred at the same time. Soil relative density can directly contribute to kinematic interaction of pile and surrounding soil.

After the beginning of shakes, earthquake waves cause deformations to occur in soil; therefore, the deformed soil applies lateral forces and bending moments to pile shaft. Dense soil, which has a higher unit weight in comparison to loose soil, would cause higher lateral influence on pile shaft. On the other hand, adjacent soil is modeled by a number of springs which are resisting against the pile lateral and axial movements thus, in a denser soil medium, more resistance exists in front of pile lateral movement. Changes in relative density have indirect impacts on pile behavior. In fact, variation in relative density would change the depth of liquefaction and consequently the free length of pile and also the depth of pile fixity.

4.3. Effect of Pile stiffness

The effects of Pile bending stiffness (EI_p) are evaluated by making variation in Pile bending stiffness from EI_{pile}=177 Nm^2 to 1450 Nm^2. The changes could reflect various kinds of pile properties, as well as possibility of cracks in piles. A constant bending stiffness of of 1450 Nm^2 has been assumed for superstructure.

M_{max} in piles with varying bending stiffness in soils with relative densities of 40%, 55%, and 80% under four seismic excitations with scaled maximum accelerations of 0.2g is presented in Fig. 7.

As shown in Fig. 7, the maximum moment, M_{max} increased with the increase in pile bending stiffness. For 93.3% of other analyzed cases, similar trend is observed. The effect of earthquake predominant frequencies is also evident from Fig. 7. It is observed that the increase in the frequency of seismic loading decreases the maximum moment, M_{max}, along pile shaft for a given a_{max}.

Figure 8 shows the development of pile bending moment through the pile shafts with different pile stiffnesses and four different earthquake frequencies with the maximum acceleration of 0.2g in medium dense sand (Dr=55%). It is evident in Fig. 8 that the depth in which the maximum value of moment, M_{max}, occurs varies with respect to variations in pile bending stiffness.

When section’s bending stiffness decreases, the amount of fixity that is creating in pile head by means of superstructure mass is becoming more predominant and the maximum bending moments takes place near the ground level. This change in depth of occurrence of M_{max} can be considered in all four earthquake excitations. When section’s bending stiffness has a value close to the stiffness of superstructure mass on pile head, the M_{max} are moved to the deeper sections of pile shaft. It can be stated that the depth of liquefaction is predominant in allocating the bending moment’s depth of happening.

4.4. Effect of unit weight of length due to changes in section

Bending stiffness and unit weight of length are changing with alteration in section geometry and kind of material. This means that with changing pile sections in order to obtain varying bending stiffness, unit weights of length are also changing. For the purpose of assessing the effect of unit weight of length on developed M_{max} in pile shaft, a section with 1 meter of diameter and a constant EI and various densities of 2500 kg/m^3, 3500 kg/m^3, and 4500 kg/m^3, is considered. The pile is embedded in medium and dense sandy soils, and is exposed to three earthquakes with maximum accelerations of 0.2g, and 0.3g.

In Fig. 9 the diagram of pile maximum moment, M_{max}, versus unit weight of length is presented for Kocaeli, Kobe, and Feriuli earthquakes in soil with relative densities of 55% and 80%. From the general trend of lines, it can be said that increase of unit weight of length of pile can change the pile bending moment slightly and the effect of variation of pile unit weight of length on M_{max} of pile is insignificant, compared to the effect of the bending stiffness of the pile section.

4.5. Effect of Pile–Soil Relative Stiffness

The previous sections have examined effects of pile stiffness and soil relative density on pile dynamic response under earthquake excitation separately. However, during earthquake and liquefaction it is necessary to consider both parameters' effects simultaneously on pile behavior. Results of several models constructed in this study implied that it is possible to define a dimensionless ratio which can provide the opportunity of considering influences regarding both claimed factors on pile bending moments. The ratio is called pile-soil relative stiffness and defined as:

$$k_r = \frac{E_p I_p}{E_s L_{eff}^4} \tag{8}$$

where E_p is modulus of elasticity of pile, I_p represents the moment of inertia of pile section, E_s stands for modulus of elasticity of soil, and L_{eff} is the depth of liquefaction plus the exposed length of pile.

The bending response of piles with exposed lengths of 1, 3, and 5 m for different pile-soil relative stiffness (k_r) under Kobe earthquake with the scaled a_{max}= 0.1g, 0.2g, and 0.3g, are depicted in Fig 10. As shown in Fig. 10, with increase in soil-pile relative stiffness, moments in piles are increased. The dimensionless soil-pile relative stiffness considers the effects of stiffnesses pertaining to the pile and soil medium, simultaneously.

5. Conclusions

Soil-pile interaction under seismic excitations has been considered in several numerical models and the influences regarding various effective parameters have been clarified. From observation and evaluation of 216 cases include 6 sections with different geometric characteristics and materials, soil with 3 various relative densities, and 4 earthquakes with predominant frequencies and maximum accelerations following conclusions have been drawn.

1. The depth of liquefaction of soil layer as well as the bending moment decrease with the increase of predominant earthquake frequency. This result is consistent with that obtained from previous findings [26]. The decrease of depth of liquefaction leads to the decrease of free length of pile.

2. In most (78.8%) of cases, increase in soil relative density increased the M_{max} in pile, which shows the denser soil impose higher moment to the pile. This important point can render the conclusion that soils with higher relative densities that may provide a desirable situation in static design may increase the risk of bending failure in seismic loading conditions.

3. Changes in pile's material and dimensions would give rise to variations in pile stiffness and unit weight of length of pile. In 93.3% of analyzed models, M_{max} increased with increase in pile bending moment. Considering the changes in unit weight of length of pile that are inevitable when the pile's bending stiffness is changed, analyses have shown that unit weight of length of pile solely have negligible effect on pile bending response.

4. In cases where the flexural stiffness of the superstructure is higher than that of the pile system, the depth on the pile length in which the maximum bending moment happens increased with increase in bending stiffness.

5. The dimensionless soil-pile relative stiffness defined in current study considers the effects of stiffnesses pertaining to the pile and soil medium and pertaining, simultaneously. With increase in soil-pile relative stiffness, moments in piles are increased.

Acknowledgement

Authors would like to appreciate the faculty members of Faculty of Civil Engineering in Babol Noshirvani Univeresity of Technology of Iran who kindly examined the research and suggested useful comments and modifications.

References

[1] Mylonakis, G., & Gazetas, G. (2000). Seismic soil-structure interaction: beneficial or detrimental. Journal of Earthquake Engineering, 4(3), 277-301.

[2] Rahmani, A., & Pak, A. (2012). Dynamic behavior of pile foundations under cyclic loading in liquefiable soils. Computers and Geotechnics, 40, 114-126.

[3] Ishihara, K. (1999). Therzaghi oration: Geotechnical aspects of the 1995 Kobe earthquake. In Proceedings of (Vol. 14, pp. 2047-2073).

[4] Tokimatsu, K.; Suzuki, H.; (1998). Effect of Inertial and Kinematic Interactions on Seismic Behaviour of Pile Foundations Based on Large Shaking Table Tests. In: Proceedings of the 2nd CUEE Conference on Urban Earthquake Engineering. Tokyo Institute of Technology (Japan).

[5] Ishihara. (2014). Lecture: An overview of the behavior of pile foundations in liquefiable and non-liquefiable soils during earthquake excitation" Soil Dynamics and Earthquake Engineering. Volume 68, January 2015, Pages 69-77.

[6] Wilson, D. W., Boulanger, R. W., & Kutter, B. L. (2000). Observed seismic lateral resistance of liquefying sand. Journal of Geotechnical and Geoenvironmental Engineering, 126(10), 898-906.

[7] Bhattacharya, S. (2003). Pile instability during earthquake liquefaction (Doctoral dissertation, University of Cambridge).

[8] Tang, L., & Ling, X. (2014). Response of a RC pile group in liquefiable soil: A shake-table investigation. Soil Dynamics and Earthquake Engineering, 67, 301-315.

[9] Abdoun, T., & Dobry, R. (2002). Evaluation of pile foundation response to lateral spreading. Soil Dynamics and Earthquake Engineering, 22(9), 1051-1058.

[10] Bolton, M. D. (2004). An alternative mechanism of pile failure in liquefiable deposits during earthquakes. Geotechnique, 54, 203-213.

[11] Yao, S., Kobayashi, K., Yoshida, N., & Matsuo, H. (2004). Interactive behavior of soil–pile-superstructure system in transient state to liquefaction by means of large shake table tests. Soil dynamics and earthquake engineering, 24(5), 397-409.

[12] Suzuki, H., Tokimatsu, K., Sato, M., & Abe, A. (2006). Factor affecting horizontal subgrade reaction of piles during soil liquefaction and lateral spreading. In Seismic performance and simulation of pile foundations in liquefied and laterally spreading ground (pp. 1-10). ASCE.

[13] Tamura, S., & Tokimatsu, K. (2006). Seismic earth pressure acting on embedded footing based on large-scale shaking table tests. In Seismic Performance and Simulation of Pile Foundations in Liquefied and Laterally Spreading Ground (pp. 83-96). ASCE.

[14] Dungca, J. R., Kuwano, J. I. R. O., Takahashi, A., Saruwatari, T., Izawa, J., Suzuki, H., & Tokimatsu, K. O. H. J. I. (2006). Shaking table tests on the lateral response of a pile buried in liquefied sand. Soil Dynamics and Earthquake Engineering, 26(2), 287-295.

[15] Jin Tae, H. A. N., Sung Ryul, K. I. M., & Jae Ik Hwang, M. M. K. (2007). Evaluation of the Dynamic Characteristics of Soil-Pile System in Liquefiable Ground by Shaking Table Tests. In: 4th International conference on earthquake geotechnical engineering. Thessaloniki, Greece.

[16] Bhattacharya, B. Tokimatsu, K. Goda, K. Sarkar, R. Shadlou, M. Rouholamin, M. (2014).Collapse of Showa Bridge during 1964 Niigata earthquake: A quantitative reappraisal on the failure mechanisms. Volume 65, Pages 55-71.

[17] Kagawa, T. (1992). Lateral pile response in liquefying sand. In Proceedings of the 10th World Conference on Earthquake Engineering (pp. 19-24).

[18] Yao, S, & Nogami T. (1994). Lateral cyclic response of piles in viscoelastic Winkler subgrade. J Eng Mech,120(4), 758-75.

[19] Fujii, S., Cubrinovski, M., Tokimatsu, K., & Hayashi, T. (1998). Analyses of damaged and undamaged pile foundations in liquefied soils during the 1995 Kobe earthquake. In Geotechnical Earthquake Engineering and Soil Dynamics III (pp. 1187-1198). ASCE.

[20] Liyanapathirana, DS, & Poulos, HG. (2005). Seismic lateral response of piles in liquefying soil. J Geotech Geoenviron Eng (1311), 1466-79.

[21] Finn, W. D. L., & Fujita, N. (2002). Piles in liquefiable soils: seismic analysis and design issues. Soil Dynamics and Earthquake Engineering, 22(9), 731-742.

[22] Klar, A., Baker, R., & Frydman, S. (2004). Seismic soil–pile interaction in liquefiable soil. Soil Dynamics and Earthquake Engineering, 24(8), 551-564.

[23] Oka, F., Lu, C. W., Uzuoka, R., & Zhang, F. (2004). Numerical study of structure-soil-group pile foundations using an effective stress based liquefaction analysis method. In 13th World conference on earthquake engineering. Canada: Vancouver (p. 3338).

[24] Uzuoka, R., Sento, N., Kazama, M., Zhang, F., Yashima, A., & Oka, F. (2007). Three-dimensional numerical simulation of earthquake damage to group-piles in a liquefied ground. Soil dynamics and earthquake engineering, 27(5), 395-413.

[25] Comodromos, E. M., Papadopoulou, M. C., & Rentzeperis, I. K. (2009). Pile foundation analysis and design using experimental data and 3-D numerical analysis. Computers and Geotechnics, 36(5), 819-836.

[26] Haldar, S., & Babu, G. S. (2010). Failure mechanisms of pile foundations in liquefiable soil: Parametric study. International Journal of Geomechanics, 10(2), 74-84.

[27] Itasca, F. L. A. C. (2000). Fast Lagrangian analysis of continua. Itasca Consulting Group Inc., Minneapolis.

[28] Byrne, P. M. (1991). A cyclic shear-volume coupling and pore pressure model for sand. In Second International Conference on Recent Advances in Geotechnical Earthquake

Engineering and Soil Dynamics (1991: March 11-15; St. Louis, Missouri). Missouri S&T (formerly the University of Missouri--Rolla).

[29] Kuhlemeyer R L, Lysmer J (1973) Finite element method accuracy for wave propagation problems. J. Soil Mech. & Foundations, Div. ASCE 99(5): 421-427

[30] Donovan, K., W. G. Pariseau and M. Cepak. "Finite Element Approach to Cable Bolting in Steeply Dipping VCR Stopes," in Geomechanics Application in Underground Hardrock Mining, pp. 65-90. New York: Society of Mining Engineers, 1984.

[31] Comodromos, E. M., Anagnostopoulos, C. T., & Georgiadis, M. K. (2003). Numerical assessment of axial pile group response based on load test. Computers and Geotechnics, 30(6), 505-515.

[32] Popescu, R., & Prevost, J. H. (1993). Centrifuge validation of a numerical model for dynamic soil liquefaction. Soil Dynamics and Earthquake Engineering, 12(2), 73-90

[33] website, www.PEER.com

Table Captions

Table1. Soil and pile properties for the validation model

Table 2. Soil properties for parametric analysis (Adapted from Haldar and Babu [26])

Table 3. Pile properties for the parametric analysis

Table 4. Earthquake data for parametric analysis [38]

Table1. Soil and pile properties for the validation model

characteristics of Soil layer	Dr=55%	Dr= 80%
Depth of soil layer, (m)	9.1	11.4
Dry unit Weight (kg/m^3)	1586	1674
Porosity	0.406	0.373
Bulk module, K (kPa)	2.92×10^5	4.05×10^5
Permeability (m/s)	6.05×10^{-5}	3.70×10^{-5}
Shear modules, G (kPa)	4.19×10^5	3.02×10^5
Poisson's ratio, υ	0.45	0.45
$(N_1)_{60}$	13	28
Friction angel, φ (^{o})	33	39
K_0	0.5	0.5
Pile elasticity modulus, E_P (GPa)	210	210

Table 2. Soil properties for parametric analysis (Adapted from Haldar and Babu [26])

Characteristics	Dr= 40%	Dr= 55%	Dr= 80%
Depth of layer, (m)	20	20	20
ρ_d (kg/m^3)	1538	1586	1674
Shear module, G (Mpa)	2.7	3.02	4.47
Bulk module, K (Mpa)	21.6	29.2	43.2
$(N_1)_{60}$	7.2	14	30
Porosity	0.424	0.406	0.373
Permeability, k (m/s)	6.6	6.05	3.7
Friction angel, φ (^{o})	33	34.2	39.5
K_0	0.5	0.5	0.5
Poisson's ratio, υ	0.45	0.45	0.45

Table 3. Pile properties for the parametric analysis

Material	Steel	Steel	Steel	Concrete	Concrete	Concrete
Diameter (m)	1	0.9	0.6	1	0.8	0.6
Thickness (mm)	t=16	t=16	t=16	_	_	_
Pile length below ground (m)	20	20	20	20	20	20
Pile length above the ground (m)	1	1	1	1	1	1
Density (kg/m^3)	7800	7800	7800	2500	2500	2500
Flexural strength, f_y (MPa)	500	500	500	11.2	11.2	11.2
Yield moment of pile in absence of axial load, (kN.m)	5987	5000	2087	1099	563	237
Yield moment of pile in presence of axial load, (kN.m)	5818	4831	1983	1005	488	181
Modulus of elasticity, E_P *(GPa)*	210	210	210	29.6	29.6	29.6
Bending stiffness, EI (Nm^2)	1260	945	273	1450	592	177

Table 4. Earthquake data for parametric analysis [33]

Earthquake	Predominant frequency(Hz)
Kocaeli.Turkey,1999,Gebze station	1.2
Kobe.Japan.1995,port island station	2.77
Friuli.Italy,1976,unknown station	3.85
Mohawk valley,Usa,2001, Silver Springs Fire Station	5

Figure Captions

Figure 1. Configuration of the finite difference model for validation

Figure 2. Excess pore-water pressure ratios at depth of 4.6 m

Figure 3. Bending moments in pile at depth of 2.3 m below ground level

Figure 4. Configuration of soil-pile system in numerical models

Figure 5. Liquefaction depth respect to predominant frequency for different soil relative densities (a) Dr = 40%, (b) Dr = 55%, (c) Dr = 80%

Figure 6. Bending moments in piles with 1 m of diameter respect to various Dr for different earthquake frequencies (a) Concrete pile, a_{max} = 0.1g, (b) Concrete pile, a_{max} = 0.3g, (c) Steel pile, a_{max}= 0.1g, (d) Steel pile, a_{max} = 0.3g

Figure 7. Variation of M_{max} respect to EI_p for four earthquakes with a_{max}=0.2g: (a) D_r = 40%, (b) D_r = 55%, (c) D_r = 80%

Figure 8. M_{max} variations respect to pile depth for a) Kobe earthquake, b) Feriuli earthquake

Figure 9. Variation of M_{max} respect to unit weight of length of pile for (a) D_r = 55%, and (b) D_r = 80%

Figure 10. M_{max} under seismic loading for different pile-soil relative stiffness (a) Frequency=2.77 Hz (b) Frequency=3.85 Hz

Figure 1. Configuration of the finite difference model for validation

Figure 2. Excess pore-water pressure ratios at depth of 4.6 m

Figure 3. Bending moments in pile at depth of 2.3 m below ground level

Figure 4. Configuration of soil-pile system in numerical models

(a)

(b)

(c)

Figure 5. Liquefaction depth respect to predominant frequency for different soil relative densities (a) Dr = 40%, (b) Dr = 55%, (c) Dr = 80%

(a) (b)

(c) (d)

Figure 6. Bending moments in piles with 1 m of diameter respect to various Dr for different earthquake frequencies (a) Concrete pile, a_{max} = 0.1g, (b) Concrete pile, a_{max} = 0.3g, (c) Steel pile, a_{max}= 0.1g, (d) Steel pile, a_{max} = 0.3g

(a)

(b)

(c)

Figure 7. Variation of M_{max} respect to EI_p for four earthquakes with a_{max} = 0.2g: (a) D_r = 40%, (b) D_r = 55%, (c) D_r = 80%

(a)

(b)

Figure 8. M_{max} variations respect to pile depth for a) Kobe earthquake, b) Feriuli earthquake

(a)

(b)

Figure 9. Variation of M_{max} respect to unit weight of length of pile for (a) D_r = 55%, and (b) D_r = 80%

(a)

(b)

Figure 10. M_{max} under seismic loading for different pile-soil relative stiffness (a) Frequency=2.77 Hz (b) Frequency=3.85 Hz

Research Highlights

- Motion of a pile in sandy soil under seismic liquefaction is considered.
- Influences of soil and pile properties on dynamic response of pile are examined.
- Pile stiffness can significantly affect the pile's dynamic response.
- Pile material densities have negligible effects on its dynamics response.
- With increase in soil-pile relative stiffness, maximum moments are increased.